Memoirs of the Faculty of Engineering, Kyushu University, Vol.69, No.1, March 2009

Terrestrial Neutrons in West Zone II Building on Ito Campus

by

Kamrun NAHER*, Nobuo IKEDA**, Hiroaki FUKUDA*, Hiroki IWAMOTO*,

Yoshinori FUKUI*, Yusuke KOBA*, Minoru IMAMURA*

and Yusuke UOZUMI***

(Received February 2, 2009)

Abstract

Thermal and fast neutrons were measured inside the West Zone II building on Ito Campus for the assessment of terrestrial neutrons in a stand alone concrete building. Ratios of count rate of thermal neutrons to that of fast neutrons were almost constant inside the building. The contribution of fast neutrons across outside wall has been discussed. A simple method to estimate the neutron flux near the outside wall has been proposed.

Keywords: Neutron flux, Single-event upset (SEU), Cosmic ray, Attenuation, Concrete shield, Building, ^{3}He counter, Neutron dose rate meter

1. Introduction

Much attention has been paid to the details of the environmental neutron flux on the ground due to the insight from the soft-fail studies of modern electronics that environmental neutrons are the prime cause of soft errors. When a charged particle produced by the neutron induced reaction hits a sensitive volume such as a depletion region (a region of unbalanced charge across a *p-n* junction) in a microelectronic device, the local carriers - electrons and holes - induced by the ionizing particle can be amplified to form an electrical pulse large enough to flip the memory state of a cell from 1 to 0 or vice versa. This random event, called a single-event upset (SEU) or soft error, causes data corruption, although it does not cause any permanent damage in the device. With development of high-tech in LSI manufacturing, its integration becomes much higher. This causes SEU to be more probable. Until recently, fast neutrons with energies greater than 1 MeV have been considered to be a main contributor to SEU. It has been pointed out, however, the use of boron as BPSG (Borophosphosilicate glass) in modern LSI manufacturing results in drastic increase of probability of SEU caused by environmental thermal neutrons, due to the huge capture cross section of the reaction $^{10}B(n,\alpha)^{7}Li$[1-4] and the energies of produced alpha (1.47 MeV) and ^{7}Li (0.84 MeV) particles sufficiently high to induce charge to cause memory flip. Therefore, information on

* Graduate Student, Department of Applied Quantum Physics and Nuclear Engineering
** Professor, Department of Applied Quantum Physics and Nuclear Engineering
*** Associate Professor, Department of Applied Quantum Physics and Nuclear Engineering

flux of both fast and thermal neutrons is of high importance.

Many experimental studies on environmental fast neutrons in high latitude area at flight altitude have been carried out in North America and Europe.[5-13] However, information on neutron flux at sea and ground levels is rather poor. Some results on cosmic ray neutrons at sea level in Japan have been reported.[14-19] A few results on cosmic ray neutrons on ground level in Japan have been available.[20, 21] In recent years, several experiments have been performed at low geomagnetic latitudes area.[14, 21] United Nations Scientific Committee on the Effect of Atomic Radiation (UNSCEAR) 2000 reported the neutron fluence rate of 47 n/cm^2-hr at sea level in high geomagnetic latitude area.[22] The values in lower geomagnetic latitude area have been reported to be lower than the UNSCEAR 2000 value.

For thermal neutrons, several authors have measured the discrepant flux values. O´brien and others have reported[23] that the measured terrestrial flux is 3 n/cm^2-hr which is 10 times larger than the theoretical prediction and discussed on the contribution of neutrons thermalized by water nearby. Later, an average flux of 106 n/cm^2-hr, about 30 times higher than the measurement by O´brien et al., has been observed by Heusser[24]. With the interest in soft fails caused by thermal neutron induced reactions in BPSG in ICs, several investigations have also been carried out. The measured fluxes range from 10 to 67 n/cm^2-hr.[1, 25] Recently, the thermal neutron flux at sea level has been measured with ^{3}He and BF_3 Boner spheres to be in the range of 1 to 4 n/cm^2-hr[21, 26]. From these prior measured values largely scattered from 1 to 300 n/cm^2-hr, it can be noted that the thermal neutron flux largely depends on terrestrial location and surroundings.

The data of neutron flux inside a concrete building is rare, while most of modern electronics are operated in the building. To the best of authors' knowledge, the available neutron flux inside the concrete building is due to Jiang and others[27] and Dirk and others.[28]. Jiang et al. measured the neutrons in a five story building with bare and polyethylene covered BF_3 counters. They have inferred that the contribution of neutrons penetrating through windows or walls to the neutron dose in the building rooms can be competitive with that passing through the roof. Dirk et al. carried out the measurement in the center of a wide six story building. Both of fast and thermal neutrons have been shown to decrease exponentially as increasing the thickness of concrete above the floor. The deduced attenuation length for thermal neutrons is about 2/3 of that for fast neutrons. Their result indicates negligible contribution of neutron across windows or walls However, it is not sure that their findings are also applicable to the case that a building is rather narrow and/or a room faces outside wall.

In the present paper, study on terrestrial neutrons in rooms of a stand alone eleven stories building is presented. The contributions of cosmic neutrons passing through the roof, window and wall are discussed.

2. Experimental Method and Results

2.1 Neutron measurement

Thermal neutrons can be detected selectively using reactions with ^{3}He, ^{6}Li, ^{10}B, or ^{235}U, which have extremely large cross sections only for neutrons in thermal energy region. Among them, the ^{3}He(n,p)T reaction has largest cross section The reaction Q value is 0.764 MeV and both of the residuals are the charged particles, so that in principle a ^{3}He counter provides signals with constant voltage corresponding to the released energy of 0.764 MeV for thermal neutrons.

Two types of the ^{3}He counters were used for neutron detection; one is of bare type for detection of thermal neutrons. ^{3}He gas is filled in a cylindrical tube with 32 cm in length and 2.5 cm in diameter. The other one is the neutron dose rate meter (NDRM), which consists of ^{3}He gas counter

of same size with the former one and 10 cm thick polyethylene surrounding the counter. The neutron dose rate meter is known to be sensitive to neutrons with energies more than 1 MeV and much less sensitive to thermal neutrons, so that neutrons with energies greater than 1 MeV are considered to be mainly measured by the NDRM . Hereafter, we define fast and thermal neutrons as those detected by the NDRM and the bare ^{3}He detector, respectively. The photograph of both the detectors and the block diagram of the electronic circuit for thermal neutron detection are shown in **Figs. 1** and **2,** respectively. Signals from ^{3}He counter were processed through preamplifier, linear amplifier and then fed to a pocket multi channel analyzer (PMCA), a timing single channel analyzer (TSCA) and a delay and gate generator (DGG) were used to produce trigger pulse for the PMCA. A personal computer (PC) was connected to the PMCA to acquire the data.

Fig. 1 Bare ^{3}He detector and neutron dose rate meter.

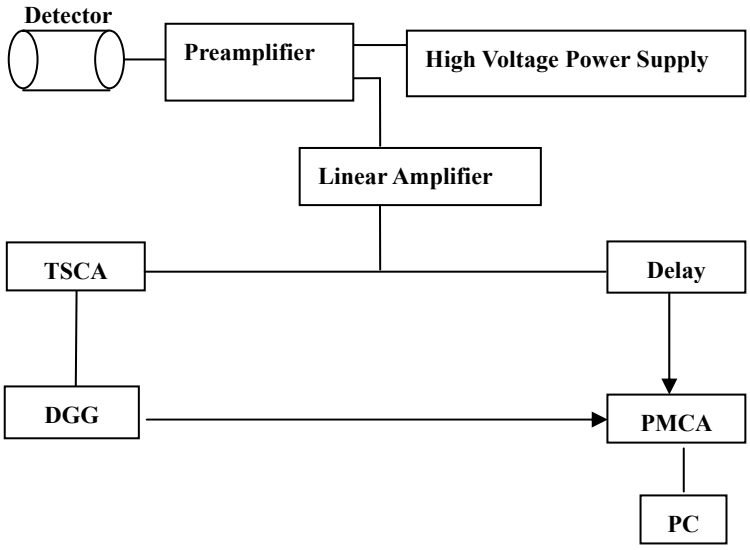

Fig. 2 Block diagram of electronic circuit with ^{3}He counter.

Measurements of neutrons were carried out in West Zone II building on Ito campus of Kyushu University, Nishi-ku, Fukuoka-shi, Japan. The height of the eleven stories building is 50 m and the thickness of the concrete floor is 15 cm, each floor has a height of about 3 m. The size of the building is about 40 m× 150 m. Measurements were conducted at 11^{th}, 9^{th}, 8^{th}, 7^{th} and 3^{rd} floors and at basement. The measurement room at basement is on the same level with the ground behind the outside wall of the room. The size and structure of the measurement rooms are not same. Rooms at 3^{rd} and 7^{th} floors and at basement are big in size and have big size window. These rooms are at the face side of the building. The room at 3^{rd} floor is located in the corner of the building and has window which covers outer side of the room, and for 7^{th} floor and basement the windows cover 50% of the outer wall. Rooms in 8^{th} and 9^{th} floors are small in size, have no window and are in the middle of the floor. One smaller building stands near the window of the room at basement. Room at 11^{th} floor is located near the end of building and its roof is not made by concrete. The building structure is shown in **Fig. 3**.

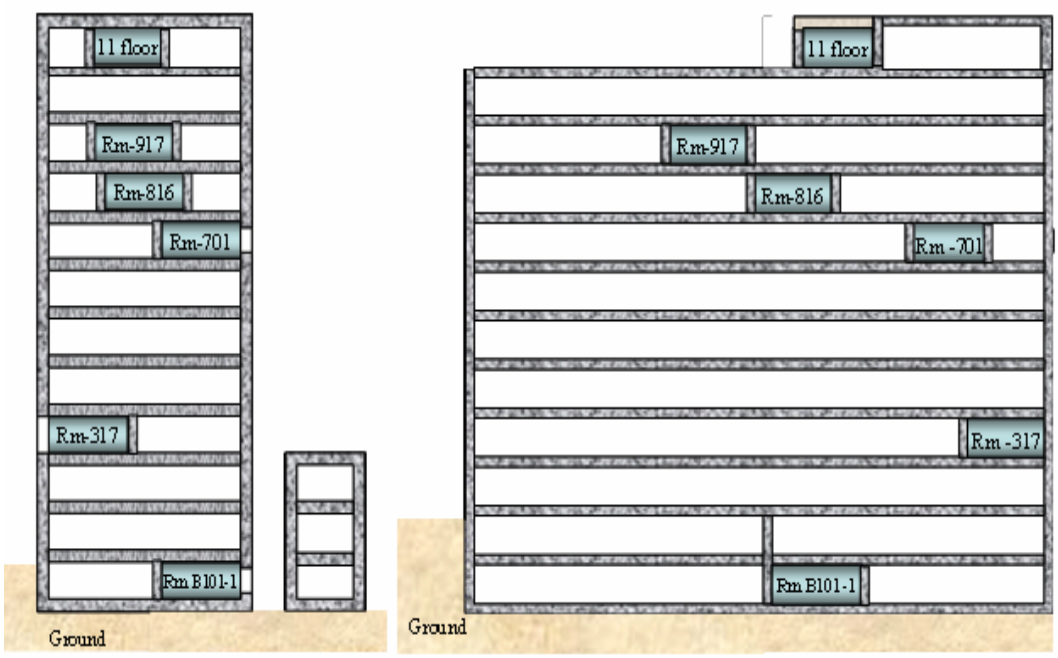

Fig. 3 Front and cross views of the West Zone II Building.

2.2 Experimental results

Measurements in each floor were repeated for four to six times in the period of 1 year. Since the rate of terrestrial neutron counting is very low, we consumed about one week in total in data acquisition for individual floors to obtain sufficient statistics. The results of the measurements of fast and thermal neutrons in different floors of the building are summarized in **Table 1**. It is to be noted in the table that the ratios of counting rate of thermal neutrons to that of fast ones are almost same for all of the floors measured, irrespective of room and window sizes and location.

Figure 4 shows the dependence of the count rates of fast and thermal neutrons on concrete thickness above the floor. The count rates attenuate exponentially in the range of concrete thickness from 15 cm to 60 cm. In the region more than 60 cm thick, however, the values are much higher than the exponential attenuation calculation to reproduce the data at 15, 45 and 60 cm.

Table 1 Measured counting rates.

Floor	Concrete thickness (cm)	Fast neutron ($\times 10^{-3}$ sec^{-1})	Thermal neutron ($\times 10^{-3}$ sec^{-1})	Ratio of thermal neutrons to fast ones
11	15	3.20 ± 0.07	45.4 ± 0.3	14.2 ± 0.3
9	45	2.07 ± 0.06	28.0 ± 0.2	13.5 ± 0.4
8	60	1.52 ± 0.05	21.0 ± 0.2	13.8 ± 0.4
7	75	1.57 ± 0.05	22.0 ± 0.2	14.0 ± 0.5
3	135	1.52 ± 0.5	21.5 ± 0.2	14.2 ± 0.5
B1	165	0.87 ± 0.04	11.2 ± 0.1	12.9 ± 0.6

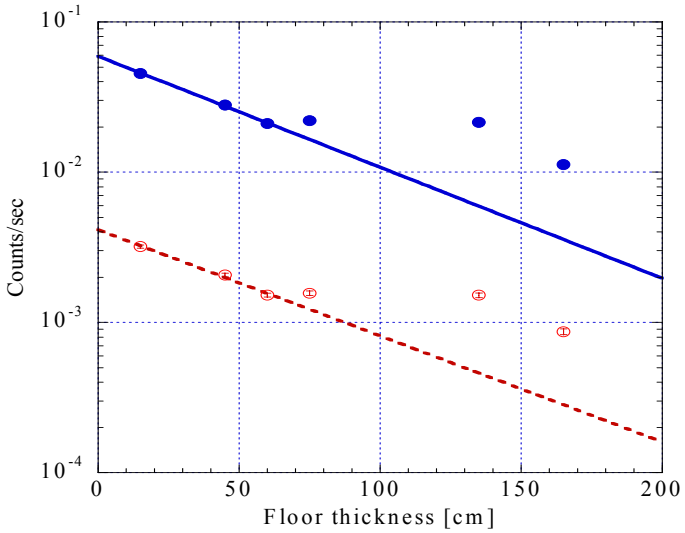

Fig. 4 Measured thermal (filled circles) and fast (open circles) neutrons count rates as a function of concrete thickness. The solid and dotted lines are the exponential function to reproduce the data at 15, 45 and 60 cm.

3. Data Analysis and Discussion

3.1 Attenuation by concrete shielding

To investigate the attenuation of neutrons due to concrete shielding, composition of concrete is desirable to be definite. Portland cement concrete is nominally a 1:2 mix of cement and sand which contains 10% water by weight. Composition of sand has variance depending on the place produced. Concrete density has been pointed out to vary up to 30%, owing to variance of composition of sand and fraction of aggregate included. Thus it is very difficult to deal with the attenuation of neutrons by concrete so that, in the following, we analyzed the data phenomenologically. We adopted the concrete density of 2.45 g/cm^3, which is the typical value for concrete used in Kyushu area.[29)]

The change in neutron count rate $N(x)$ by concrete thickness x can given by

$$N(x) = N_n^0 \exp(-\mu x) \tag{1}$$

where N_n^0 is the neutron count rate before absorption by concrete, and μ the neutron attenuation

coefficient. The attenuation length ($1/\mu$) deduced by using the fast neutron data at 11th to 8th floors (solid line in **Fig. 4**) is 149 g/cm^2, which is in reasonable agreement with previous investigations.[28, 30] This agreement, together with the large deviation of the data at lower floors from exponential behavior, strongly suggests the contribution of some neutrons other than passing through the roof, on lower floors.

3.2 Window and wall effect on fast neutron fluxes

As suggested in Ref. 27), sky neutrons are possible to come into rooms by passing through windows or walls. It is important to clarify their contribution at each measurement location.

We consider number of fast neutron counted per unit time $C(x)$ to be represented as follows,

$$C(x) = A_1 \exp(-\mu x) + A_2 \tag{2}$$

where A_1 is the flux, measured at roof, of neutrons which reach to the room by passing through the concrete floors, and A_2 is the flux, measured in the room, of neutrons passing through the window or the wall. We assumed for simplicity that the attenuations of neutrons by wall and window are negligibly small. This assumption leads to the criterion that $A_1 + A_2$ should be exactly same for all of the floors. We first determined the μ , A_1 and A_2 values for the neutron counting rates at 7th and 11th floors and at basement, on the assumption that the same A_1 and A_2 values can be applied to the measurement rooms facing the outside wall. The deduced attenuation length is 140 g/cm^2, which is in reasonable agreement with Refs. 28) and 30) Using thus obtained attenuation length and the $A_1 + A_2$ value, the individual A_1 and A_2 values were determined for all of the other floors. The deduced A_1 and A_2 values at different floors are shown in **Table 2** together with the measured and calculated count rates.

The $A_2/(A_1 + A_2)$ value of 17.3% deduced from the data at 11th and 7th floors and at basement is considered to be possible to apply for rooms facing outside wall in the other stand alone buildings, although some deviation may be caused by the structure of the building such as the thickness of the outside wall. The smaller $A_2/(A_1 + A_2)$ values were deduced for 8th and 9th floors. These variations are reasonable because the measured rooms are located in the center of the building and have no window. The reason of the differences in $A_2/(A_1 + A_2)$ values between 8th and 9th floors is not clear but it is sure that the measured room at 9th floor is somewhat closer to the outside wall than that at 8th floor. The $A_2/(A_1 + A_2)$ value for 3rd floor is about twice of those for 11th and 7th floors and for basement. This is quite reasonable because the measured room at 3rd floor is located in the corner of the building so that two sides face the outside wall.

Table 2 Measured and calculated fast neutron count rates with the value of A_1 and A_2 .

Floor	Concrete thickness (cm)	Measurement ($\times 10^{-3}$ sec^{-1})	Calculation ($\times 10^{-3}$ sec^{-1})	A_1 ($\times 10^{-3}$ sec^{-1})	A_2 ($\times 10^{-3}$ sec^{-1})	$\frac{A_2}{A_1 + A_2}$ (%)
11	15	3.20 ± 0.07	3.20	3.270	0.685	17.3
9	45	2.07 ± 0.06	2.07	3.465	0.490	12.4
8	60	1.52 ± 0.05	1.52	3.747	0.208	5.3
7	75	1.57 ± 0.05	1.57	3.270	0.685	17.3
3	135	1.52 ± 0.5	1.52	2.692	1.263	31.9
B1	165	0.87 ± 0.04	0.86	3.270	0.685	17.3

Figure 5 shows a comparison of the calculation using A_1 and A_2 deduced from the data at 11th and 7th floors and at basement with the measured fast neutron count rates. The individual contributions of neutrons passing through the wall (window) and the roof are also shown. From this figure, it is clear for the rooms facing the outside wall that neutrons across the wall become more contributive than those from the roof when the thickness of concrete above the room is greater than 95 cm.

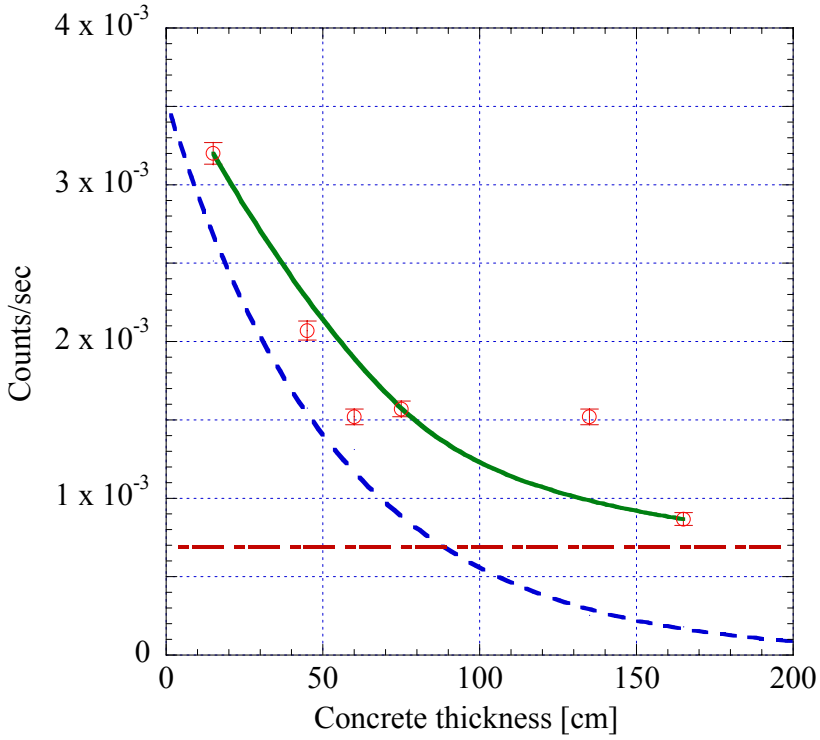

Fig. 5 Comparison of measured count rates of fast neutrons with calculation for the rooms facing outside wall (solid line). The dashed and dot-dashed curves are the individual contributions of neutrons passing through roof and wall (window), respectively.

3.3 Thermal neutron flux

The thermal neutron data were analyzed in the same procedure as described in sect. 3.2. **Figure 6** shows a comparison of the calculation using A_1 and A_2 deduced from the thermal neutron data at 11th and 7th floors and at basement with the measured thermal neutron count rates, together with the individual contributions of neutrons passing through the wall (window) and the roof. The deduced A_1 and A_2 values tabulated in **Table 3** indicate that neutrons passing through the outside wall are in general less contributive than the case of fast neutron. It is to be noted in the calculated results for 8th and 9th floors that neutrons across the outside wall make negligible contribution toward the neutron flux in rooms in the center of the buildings. The attenuation length deduced by the analysis using the thermal neutron data at 11th and 7th floors and at basement is 148 g/cm^2, almost the same with that obtained for fast neutrons. This result is contradictory to the observation by Dirk and others.[28] They measured the flux in the center of the wide building and found that the attenuation length for thermal neutrons is about 102 g/cm^2, much lower than our result. As

described in section 1, the thermal neutron flux is possible to largely depend on surroundings. Further investigations will be necessary to give more insight on the flux of thermal neutrons in the buildings.

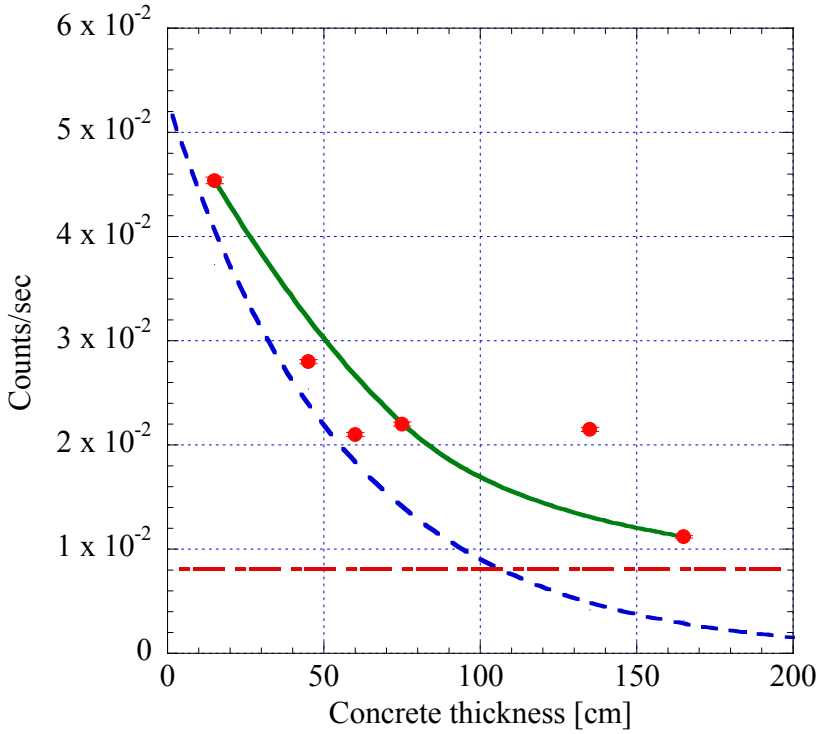

Fig. 6 Comparison of measured count rates of thermal neutrons with calculation for the rooms facing outside wall (solid line). The dashed and dot-dashed curves are the individual contributions of neutrons passing through roof and wall (window), respectively.

Table 3 Measured and calculated thermal neutron count rates with the value of A_1 and A_2 .

Floor	Concrete thickness (cm)	Measurement ($\times 10^{-3}$ sec^{-1})	Calculation ($\times 10^{-3}$ sec^{-1})	A_1 ($\times 10^{-3}$ sec^{-1})	A_2 ($\times 10^{-3}$ sec^{-1})	$\frac{A_2}{A_1 + A_2}$ (%)
11	15	45.4 ± 0.3	45,4	47.8	8.1	14.5
9	45	28.0 ± 0.2	28.0	53.3	2.6	4.7
8	60	21.0 ± 0.2	21.0	55.5	0.4	0.7
7	75	22.0 ± 0.2	22.0	47.8	8.1	14.5
3	135	21.5 ± 0.2	21,5	38.6	17.3	30.9
B1	165	11.2 ± 0.1	11.2	47.8	8.1	14.5

4. Conclusion

We measured the count rates of thermal and fast neutrons by using bare ^{3}He counter and neutron dose rate meter, respectively, for the assessment of terrestrial neutrons in a concrete building. A simple method to roughly estimate the neutron flux in rooms facing the outside wall has been proposed. It has also been pointed out that, in the rooms in the center of the building, neutrons across the outside wall are less contributive than the case facing the outside wall. Investigation on the neutron flux in various locations in individual floors is needed to provide a tool for estimating the neutron flux at any position. However, it is difficult to find rooms which allow long-term measurements without disturbance in the West Zone II building. The measurements in the other buildings combining with the purpose of examining applicability of the proposed estimation method might be desirable.

References

1) R. Baumann, T. Hossain, E. Smith, S. Murata, and H. Kitagawa; Boron as primary source of radiation in high density DRAM"s, Proc. IEEE VLSI Technology Symp., Kyoto, Japan, pp. 81-82 (1995).
2) R.C. Baumann, T.Z. Hossain, S. Murata, and h. Kitagawa; Boron compounds as a dominant source of alpha particles in semiconductor devices, Proc. 33rd Annu. IEEE IRPS, Las Vegas, NV, pp. 297-302 (1995).
3) R.C. Baumann and E. B. Smith; Neutron induced ^{10}B fission as a major source of soft errors in high density SRAM"s, Microelectronics Reliability, Amsterdam, The Netherlends: Elsvier, vol. 41, pp. 211 (2001).
4) Neutron-induced boron fission as a major source of soft errors in deep submicron sram devices, Proc. IEEE IRPS, San Jose, CA, pp. 297 (2000).
5) M. Florek, J. Masarik, I. Szarka *et al.*; Natural neutron fluence rate and the equivalent dose in localities with different elevation and latitude, Radiat. Prot. Dosim., vol. 67, no.3, pp. 187-192 (1996).
6) H. Schraube, J. Jakes, A Sannikov *et al.*; The cosmic-ray induced neutron spectrum at the summit of the zugspitze (2963 m), Radiat. Prot. Dosim., vol. 70, no. 1-4, pp. 405-408 (1997).
7) H. Schraube, V. Mares, S. Roesler *et al.*; Experimental verification and calculation of aviation route doses, Radiat. Prot. Dosim., vol. 110, no. 1-4, pp. 387-392 (2004).
8) P. Goldhagen, M. Reginatto, T. Kniss *et al.*; Measurement of the energy spectrum of cosmic-ray neutrons abroad an ER-2 high-altitude airplane, Nucl. Instrum. Methods A., vol. 476, pp 42-51 (2002).
9) M. Hajek, T. Berger, W. Schoener *et al.*; Analysis of the neutron component at high altitude mountains using active and passive measurement devices, Nucl. Instrum. Methods A., vol. 476, pp 52-57 (2002).
(10) B. Wiegel, A. V. Alevra, M. Matzke *et al.*; Spectrometry using the PTB neutron multisphere spectrometer (NEMUS) at flight altitude and at ground level, *Nucl*. Instrum. Methods A., vol. 476, pp 69-73 (2002).
11) A.M. Romero, J.C. Seaz-Vergara, R. Rodriguez *et al.*; Study of the ratio of non-neutron to neutron dose components of cosmic radiation at typical commercial flight altitudes, Radiat. Prot. Dosim., vol. 110, no. 1-4, pp. 357-362 (2004).
12) M.S Gordon, P. Goldhagen, K.P. Rodbell, T.H. Zabel, H.H.K. Tang, J.M. Clem, and P. Bailey; Measurement of the flux and energy spectrum of cosmic ray induced neutrons on the ground, IEEE

Transactions on Nuclear Science, Vol. 51, No. 6, pp. 3427-3434 (2004).
13) P. Goldhagen, J.M. Chem, and J.W. Willson; The energy spectrum of cosmic-ray induced neutrons measured on an airplane over a wide range of altitude and latitude, Radiat. Prot. Dosim., vol. 110, no. 1-4, pp. 387-392 (2004).
14) T. Nakamura, Y. Uwamino, T. Okubo *et al.*; Altitude variation of cosmic-ray neutrons, Health. Phys., vol. 53, no. 5, pp 509-517 (1987).
15) T. Nakamura, T. Nunomiya, S. Abe, K. Terunuma and H. Suzuki; Sequential measurement of cosmic ray neutron spectrum and dose arte at sea level in Sendai, Japan, J. Nucl. Sci. Technol., vol. 42, no. 10, pp 843-853 (2005).
16) M. Kowatari, K. Nagaoka, S. Satoh, Y. Ohta, J. Abukawa, S. Tachimori and T. Nakamura; Evaluation of the altitude variation of the cosmic-ray induced environmental neutrons in the Mt. Fuji area, J. Nucl. Sci. Technol., vol. 42, no. 6, pp 495-502 (2005).
17) M. Kowatari, Y. Ohta, K. Nagaoka, S. Satoh, K. Nagaaoka, J. Abukawa and T. Nakamura; Evaluation of geomagnetic latitude dependence of the cosmic ray induced environmental neutrons in Japan, J. Nucl. Sci. Technol., vol. 44, no. 2, pp 114-120 (2007).
18) T. Nunomiya, S. Abe, N. Hirabayashi *et al.*; Sequential measurements of cosmic-ray neutron induced and ambient dose equivalent on the ground, Nucl. Instrum. Methods A., suppl. 4, pp. 466-469 (2000).
19) K. Nagaoka, M. Kowatari, S. Satoh *et al.*; Altitude and latitude variations in the environmental neutron dose rate in Japan, Hoken Butsuri, vol. 39, no. 4, pp 352-361 (2004).[In Japanese]
20) C.Y. Chen, C. Chung; Low intensity cosmic neutron measurements using a portable BF_3 counting system, Nucl. Instrum. Methods A., vol. 395, pp 195-201 (1997).
21) R.J. Sheu, S.H. Jiang; Cosmic-ray induced neutron spectra and effective dose rates near air/ground and air/water interfaces in Taiwan, Health. Phys., vol. 84, no. 1, pp 92-99 (2003).
22) United Nations Scientific Committee on the Effects of Atomic Radiation, Sources and effects of ionizing radiation, *UNSCEAR* 2000 report to the general assembly, with scientific annexes, 1, United Nations Publication, New York (2000).
23) K. O´ brien, H.A. Sandmeier, G.E. Hansen, and J.E. Campbell, J. Geophys. Res., vol. 83, p 1114 (1978).
24) G. Heusser; The background components of germanium low-level spectrometers, Nucl. Instrum. Methods, vol. B17, pp. 418-422 (1986).
25) R. Baumann; Soft error characterization and modeling methodologies at Texas instruments, Presented at Proc. Semiconductor Research Council 4th Topical Conf. Reliability. [CD-Rom] SemaTech CD-ROM 0043-3283.
26) P. Goldhagen; Overview of aircraft radiation exposure and recent ER-2 measurements, Health Phys., vol. 79, pp. 526-544 (2000).
27) S. H. Jiang, J.J. Yeh, R.Y. Lin, *et al.*: A Study on Natural Background Neutron Dose, IEEE Trans. Nuclear Science, Vol. 41, No. 4, pp.993-998 (1994).
28) J.D. Dirk, M.E. Nelson, J.F. Ziegler, A. Thompson, T.H. Zabel; Terrestrial thermal neutrons, IEEE Transactions on Nuclear Science, Vol. 50, No. 6, pp.2060-2064 (2003).
29) T. Tomimasu; private communications.
30) J.F. Ziegler;Terrestrial cosmic rays, IBM J. Res. Develop, Vol. 40, No. 1, 19 (1998), and references therein.